Hygrothermal, mechanical and durability assessment of vegetable concrete mixes made with Alfa fibers for structural and thermal insulating applications

Mouatassim Charai, Ahmed Mezrhab, Ligia Moga, Mustapha Karkri

HAL Id: hal-04316674
https://hal.u-pec.fr/hal-04316674

Submitted on 22 Jul 2024

1 **Hygrothermal, mechanical and durability assessment of vegetable concrete mixes made with**
2 **Alfa fibers for structural and thermal insulating applications**

3 Mouatassim Charai [a, b *], Ahmed Mezrhab [a], Ligia Moga [c], Mustapha Karkri [b]

4 [a] Laboratory of Mechanics and Energy, Mohammed 1st University, 60000 Oujda, Morocco
5 [b] Univ Paris Est Creteil, CERTES, F-94010 Creteil, France
6 [b] Civil Engineering and Management Department, Technical University of Cluj-Napoca, 400027
7 Cluj-Napoca, Romania

8 *corresponding author:*
9 Email: charai.m@yahoo.com, charai_mouatassim1718@ump.ac.ma |Phone: +212 611683100|
10 ORCID: 0000-0003-0510-9016 | BV Mohamed VI BP 717, Mohammed First University, Faculty of
11 Sciences, 60000 Oujda, Morocco

12 **Abstract**.
13 This paper focuses on developing suitable concrete composites incorporating Alfa fibers
14 (AF) for use in insulation and structural applications. Five formulations were prepared
15 using AF weight ratios ranging from 0–10wt%. The mixtures' performance was assessed in
16 terms of thermal insulation, compressive and flexural strengths, abrasion, moisture
17 sorption, and buffering capacities. The results show that increasing AF contents improve
18 concrete's thermal insulation and sorption capacities while reducing its mechanical
19 strengths. Whereas the durability tests highlight the reinforcement character of AF,
20 revealing that an incorporation range of 0–5wt% improves the abrasion resistance.
21 Formulations with 5wt% and 10wt% AF resulted in vegetable concretes with an average
22 compressive strength of 3.78–0.6 MPa, and a thermal conductivity value of 0.46–0.19
23 W/mK, respectively. Moreover, MBV tests showed that both mixtures are classified as
24 "EXCELLENT" moisture regulators; therefore, they are appropriate as structural and
25 insulating building materials with improved hygrothermal properties.

26 **Keywords.**
27 Bio-based lightweight concrete; Thermal conductivity; Abrasion; Hygrothermal properties;
28 Compressive strength; Sustainability.

29 **Highlights**
30 • Alfa fibers (AF) as a green aggregate for structural/insulating vegetable concrete.
31 • Effect of AF contents on hygrothermal and mechanical properties of concrete.
32 • The addition of 2-5wt% AF improves the abrasion resistance of concrete.
33 • AF-based concrete formulations are suitable for structural and insulating building components.
34 • Novel bio-sourced concrete with excellent moisture buffer capacity.

1 **Nomenclature**

2 A   area (m^2)

3 F   maximum load (N)

4 m masse (kg)

5 MBV   moisture buffer value ($g/(m^2.\%RH)$)

6 R_c compressive strength (MPa)

7 R_f flexural strength (MPa)

8 V volume (m^3)

9 vol%   volume percent

10 wt%   weight percent

11 η_{eff} effective porosity (%)

12 λ thermal conductivity (W/m.K)

13 ρ density (kg/m^3)

14 φ relative humidity (-)

15 ω water content (kg/kg)

16 *Subscripts and superscripts*

17 ads adsorption

18 d dry

19 des desorption

20 w wet

21 s sample

22 j ads or ads

23 *Acronyms*

24 AF   Alfa fibers

25 AFC   Alfa fiber concrete

26 LWC   Lightweight concrete

1   Introduction

Lightweight concrete (LWC) incorporating plant fibers is emerging as a trendy promising technique among scholars and construction professionals to design eco-efficient materials for low-carbon buildings. Over the past decade, many plant fibers such as date palm [1], sugarcane [2], cork [3], and straw [4] have been successfully tested as agro-aggregates for bio-based LWC concrete. These kinds of cost-effective, natural, and renewable additives have been demonstrated to play a substantial role when added in appropriate quantities to standard binders (i.e., cement and lime), primarily in terms of (i) carbon footprint mitigation (ii) mechanical stabilization, and (iii) hygro-thermo-acoustic insulation.

Plant fibers in the concrete manufacturing process can result in low embodied carbon building envelopes, which can even operate as a carbon sink. Indeed, ~1 kg of bio-based building materials can store at least ~1.44 kgCO2e at a 12% relative humidity level [5]. Furthermore, at the building scale, walls built of 0.25 m hemp concrete blocks can sequester 14–35 kgCO2e/m^2 over a 100-year lifespan [6]. This is why the use of plant fibers as agro-agregates for concrete could be benefical, mainly when applied to ordinary Portland cement (OPC), which presents an alarming issue as it accounts for 7% of global CO2 releases and 12–15% of the overall industrial energy consumed worldwide.

From a thermal insulation point of view, all studies on vegetable concrete in the literature have shown lower thermal conductivity values ranging from 0.06–0.2 W/mK [7], compared to conventional values (0.76–1.37 W/mK) [8]. Generally, this is attributed to the low thermal conductivity of plant fibers and the high-generated porosity of plant-based concrete. Moreover, the inclusion of plant fibers in the building elements can delay heat transfer across the building envelope, resulting in significant reductions in the heating and cooling needs [9, 10]. Speaking of energy savings in numbers, a recent study by [11] indicated that employing straw bales as a construction material can cut building energy usage and embodied carbon releases by 83.12% and 76%, respectively. These results are generally in line with observations of most research on bio-based concrete buildings (see Ref. [10], [12], [13]). These include, for example, Strandberg-de Bruijn et al. [12] who demonstrated the benefit of such composite walls in reducing space

heating by 33% compared to traditional walls. More, Le et al. [13] reported the potential of hemp concrete, when compared to cellular concrete, to mitigate 15–45% of the annual energy consumption depending on the adopted ventilation strategy. For all of these reasons, plant-based concrete could be a viable alternative for achieving global carbon neutrality while also lowering construction costs and the building industry's fast-expanding energy demand.

Aside from sustainability and thermal performance, various studies have been recently oriented towards studying the effect of plant fibers on improving the hygric features of concrete. The findings have shown that vegetable concrete exhibits excellent hygrothermal properties and contributes very well to indoor comfort and healthy built constructions. Indeed, it should be noted that all published researches proved the efficacy of plant fibers incorporation in designing lightweight concrete composites classified as excellent moisture regulators [7]. At the building level, Aversa et al. [14] carried out in-situ measurements on two buildings constructed with hemp-based concrete blocks. They found that used bio-based concrete has a good hygrothermal performance, offering well inside comfort even when the outdoor climate conditions are unstable. Similar findings were reported in [15], [16], highlighting the effectiveness of vegetable concrete in damping the fluctuations of temperature and relative humidity in buildings.

Among aggregates of plant origin, Alfa (*Stipa tenacissima L.*) fibers have recently piqued the interest of the scientific communities in North Africa working in the field of bio-based composites and green buildings. In fact, the low thermal conductivity (0.042 W/mK), the good mechanical characteristics, the high cellulose content (45%), and the local availability (e.g. approximately 3.1 million hectares in Morocco) have led Alfa fibers to be tested for the manufacture of next-generation building materials with improved thermal [17] and acoustic [18] properties.

Until now very few studies have been conducted on vegetable concrete containing Alfa fibers (AF): most of them deal with thermal and mechanical performances [17], [19], one on hydration kinetics [20], and a more recent study on life cycle assessment and environmental impact analysis of Alfa fibers in concrete production [21]. They indicate that an incorporating rate of 1% of short AF is recommended for improving the mechanical strength of concrete;

4

considerable thermal insulation obtained with increasing AF contents; AF reinforced concretes showed a strong benefit in climate change mitigation.

There is no previous research on the hygrothermal characterization of vegetal concrete incorporating Alfa fibers despite the crucial impact of the hygric properties on the overall comfort in buildings. The purpose of this study, thus, is to firstly investigate the impact of AF contents on the thermomechanical performances of cement-based concrete and give recommendations for appropriate formulations for future construction uses. Thereafter, the hygric (thermal sorption isotherms and the moisture buffering capacity) characteristics of selected formulations were experimentally studied.

For comparison reasons, the mix proportion design is based on the work of Benmansour et al. [1], where studied the potential use of date palm fibers (DPF) in producing bio-based concrete mixtures for structural and insulation purposes based on the RILEM functional classification of lightweight concrete [22]. Note that the optimal mix obtained (i.e., 15wt% DPF cement-based mixture) was the subject of a research paper by Chennouf et al. [23] who focused on the hygrothermal performance of the selected mixture. Combining the objectives of the above research studies, this paper seeks to characterize the most relevant hygrothermal and mechanical properties of innovative concrete formulations incorporating AF fibers as plant aggregates. The micro-morphology, microcrystalline structure, thermal stability and porosity of AF were also identified using scanning electron microscopy (SEM), X-ray diffractometry (XRD), thermal gravimetric (TG) analysis, and liquid pycnometer technique, respectively. This study is the first paper to identify the hygric features of such a sustainable material. Furthermore, this paper also provides some new data related to next-generation concrete composites, primarily regarding hygrothermal properties and appropriate applications for energy efficiency in buildings.

2 Materials and formulations design

2.1 Raw materials, origin and identification

Bio-composites developed in this work were made with different proportions of sand, cement, and Alfa plant (*Stipa tenacissima L*) fibers. The binder is a commercial ordinary Portland cement

type (StructoPlus®; CEM II/B-M(S-LL) – 42,5R) supplied by LafargeHolcim (Romania) S.A. The used Portland cement CEM II – 42,5R meets the technical requirements as specified in the Europen standard NF EN 197-1: 2012 [24]. The natural sand used was delivered from the gravel pit from Beclean, Bistriţa County of Romania, with a maximum size of 1 mm. Fig. 1 shows sand particle size distribution in compliance with the standard test NF EN 1015-1 [25]. The main chemical elements of both cement and sand are determined using X-Ray fluorescence (XRF) analysis. The obtained results are reported in Table 1.
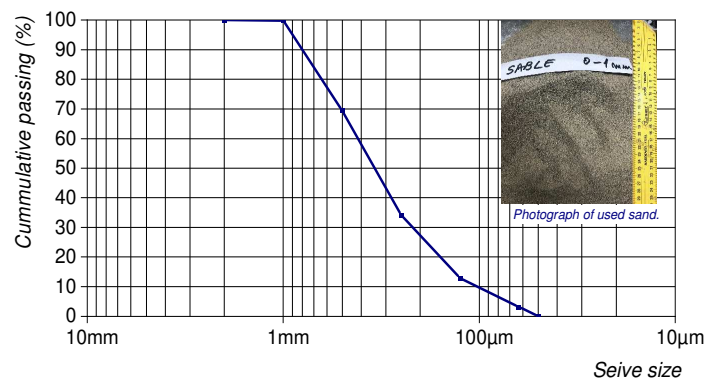
Fig. 1. Size distribution of used sand (0 – 1 mm).

Table 1. Chemical composition of cement and sand (content in %).

Oxides	Cement	Sand
CaO	60.53	0.57
SiO_2	10.94	84.96
AL_2O_3	1.55	9.64
Fe_2O_3	7.18	0.06
MgO	-	0.41
SO_3	2.09	0.01
K_2O	1.29	0.09
MnO	0.29	0.33
TiO_2	0.70	1.66
P_2O_5	-	0.01
ZnO	0.03	-

Alfa fibers (AF) were collected from the surroundings of Jerada City, eastern Morocco. The main chemical composition of Moroccan AF is given in [26]. The other physical characteristics of AF are reported in [27].

Since the thermal insulation quality of building materials is directly linked to the porosity property, the true density and porosity of cement and AF were determined using the liquid

pycnometer technique. The measurements were performed on three samples in accordance with the NF EN ISO 1183-1 [28]. Table 2 shows the obtained results. It can be clearly concluded that Alfa fibers have higher porosity compared to cement, highlighting the potential use of AF to enhance the thermal insulation of cement-based composites.

Table 2. Porosity and true density of the used materials.

Raw material	$\rho_{apparent}$ [g/cm^3]	ρ_{true} [g/cm^3]	η [%]
Cement	1.75	2.27	23.0
AF	0.63	1.25	49.6

The microscopic morphology of AF was visualized using a field emission scanning electron microscope (SEM; FEI, Quanta FEG-450). Fig. 2 shows the microstructure of AF exhibiting microfibrils with porous structures, which indicates the potential use of AF as a pore-forming agent for plant-based LWC concrete.
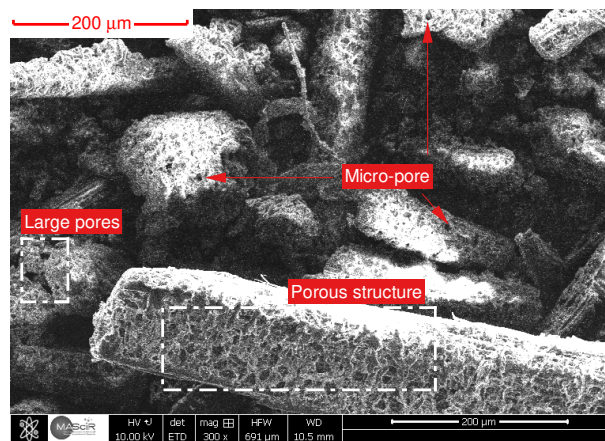

Fig. 2. SEM micrograph of raw AF.

To evaluate the AF's microcrystalline structure, X-ray diffraction (XRD) analysis was also performed on crushed raw AF samples using a SHIMADZU XRD-6000 diffractometer (λ=0.154 nm, Cu-Ka radiation), with a scan rate of 2°/min at a 2θ-scale between 5° and 40°. In addition, the thermal degradation n behaviors of AF were evaluated using a thermal gravimetric (TG) analyzer (Shimadzu, DTG-60) under an air atmosphere between 30 to 700 °C at a constant heating rate of 10 °C/min.

The XRD and TG-DTG curves of used raw AF are displayed in Fig. 3. The profiles obtained are in line with those reported by El Achaby et al. [29]. The XRD pattern (Fig. 3a) appeared four prominent peaks at 2θ of 15.3°, 16.8°, 22.3°, and 37.7°, indicating cellulose I: (1$\bar{1}$1), (110),

7

1   (200) and (004) crystallographic planes, respectively. According to the empirical Segal method

2   [30], Fig. 3a also indicates that raw AF fibers have a crystallinity index (CrI) value of 48.3%. The

3   obtained CrI is in good agreement with the values reported in the literature (e.g., [29], [31]).

4   Fig. 3b shows TG-DTG thermographs of AF, highlighting three main weight loss stages, as for

5   natural fibers of plant origin [32]: water evaporation ($\sim$90°C), cellulose I decomposition

6   ($\sim$320°C) and lignin degradation ($\sim$470°C).
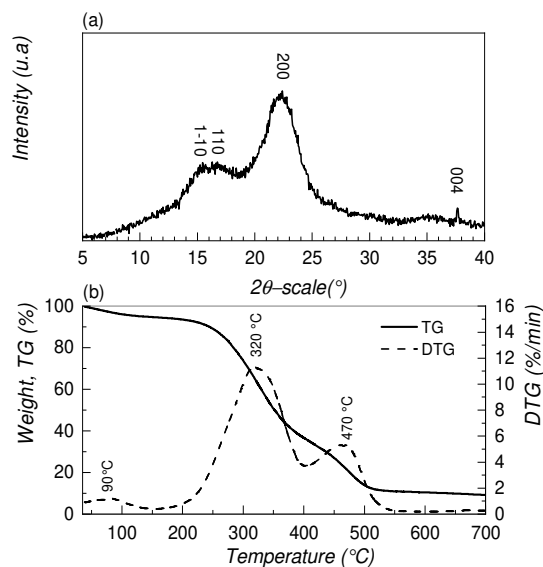
7
8   **Fig. 3.** XRD (a) and TG-DTG (b) patterns of raw AF.

9   2.2 Formulations and mix proportions

10 Five different AF dosage combinations ranging from 0–10wt% were investigated to evaluate the

11 impact of AF contents on the performance of bio-concrete. The formulation of each mixture is

12 reported in Table 3. As previously stated, the design of the mix proportions was inspired by the

13 work of Benmansour et al. [1] to ensure the comparability of the test findings. Their research

14 has been devoted to evaluating the influence of incorporating up to 30wt% of date palm fibers

15 on concrete's thermal and mechanical properties. Note that a maximum incorporation rate of

16 10wt% was considered in this study due to the AF's relatively rigid nature.

17 Before preparation, Alfa plant stems were manually cut into 30 mm long fibers. Then the

18 prescribed fiber content was gradually added after approximately 5 min of wet mixing of

19 cement and sand with water. A water-to-cement ratio of 1:2 was used for all the mixes. In this

20 study, the specimens without fiber addition consist the reference samples. A concrete mixer

machine with a speed of 300 rpm was used to achieve homogeneous mixtures. The prepared formulations were then poured into greased molds, which were placed on a vibrating table (shown in Fig. 4a) to avoid air bubbles and improve the surface finish of the material. Finally, the specimens were dried under ambient conditions (Fig. 4b) until the testing time.

Table 3. Mix design of AFC composites (% by weight).

Mix	Cement	Sand	AF [a]	w/c
AFC0	85	15	0	0.5
AFC2	70	28	2	0.5
AFC5	69	26	5	0.5
AFC7	68	25	7	0.5
AFC10	66	24	10	0.5
w/c: water-to-cement ratio				
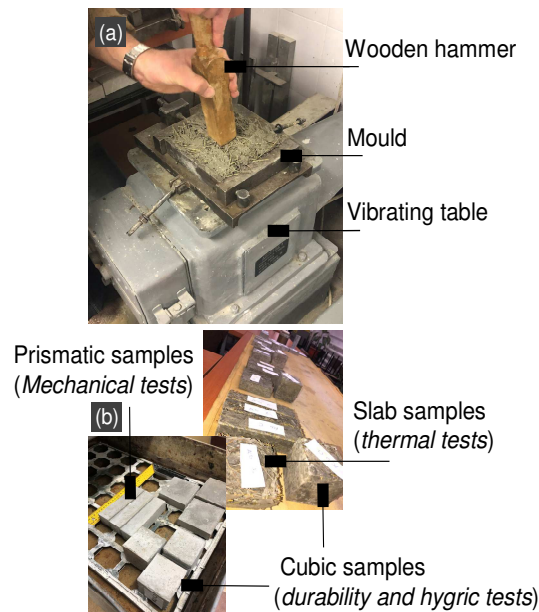
Fig. 4. Sample preparation (a) protocol (b) specimens at the age of 7 days.

In order to succeed the experimental protocols for the various tests (see further Table 4 for test specifications), specimens of different shapes were produced (Fig. 4b), namely: slab specimens (100 × 100 × 30 mm³) for measuring the thermal conductivity, prismatic samples (160 × 40 × 40 mm³) for mechanical properties testing, and cubic specimens (71 × 71 × 71 mm³) for evaluating the abrasion resistance and water absorption. To ensure that the hygrothermal results are representative, both prismatic and cubic samples were used for evaluating the hygric properties of AFC composites. Photographs of prepared AFC composites at 28 days are displayed in Fig. 5.
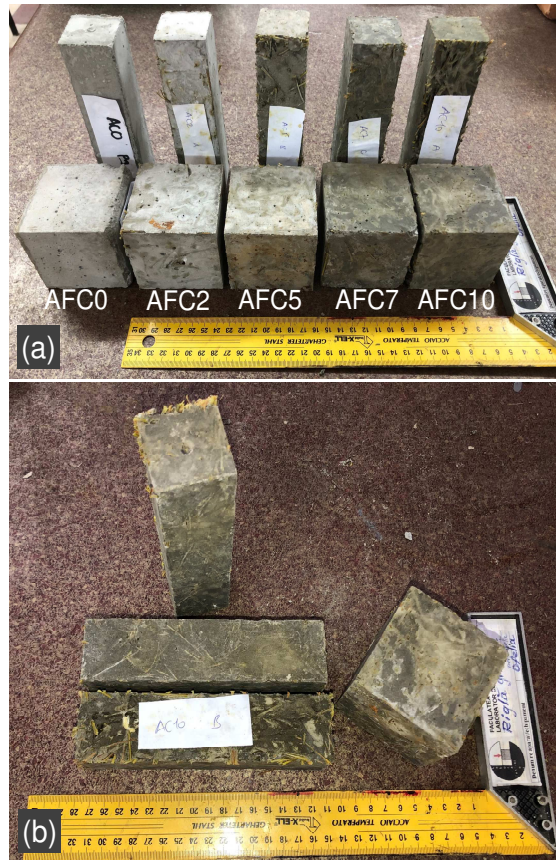
Fig. 5. Photographs of prepared specimens (a) AFC mixes (b) AFC10.

3   Characterization techniques

For the sake of clarity, all test experiments considered in this work and their standard specifications are summarized at the end of this section, i.e., in Table 4.

3.1 Apparent density and effective porosity

The apparent density of bio-based composites was measured at the age of 28 days from the measurement of the dry sample mass and specimen size, as specified in the French standard NF EN 12390-7 [33]. The weightings were performed on a balance with an accuracy of ±0.01g, while the specimen size was determined using a digital vernier caliper with a least count of ±0.05 mm.

Porosity property is one of the key factors affecting the thermal insulation quality of materials. Thus, the effective porosity was determined on dry cubic samples (71x71x71 mm^3 of dimensions) as discussed by Lian et al. [34]. The tested specimens were firstly oven-dried at 105±5 °C until they reached constant weight and then immersed in water for 24 h. The effective

porosity was measured by assessing the volume of water displaced by specimens using the following expression:

$$\eta_{eff} = 100 \times \frac{V_{app} - V_w}{V_{app}} \tag{2}$$

η_{eff} is the effective porosity, in %, V_{app} is the apparent volume of samples, in m³, V_w is the volume, in m³, of water absorbed by the open pores as defined in [34].

3.2 Mechanical properties

3.2.1 Flexural strength

Strength tests of specimens were established at the age of 28 days according to EN 196-1:2016 [35]. Firstly, the flexural strength was carried out on three 160x40x40 mm³ prisms for each mix by the three-point bending technique using an automatic flexural tensile L15 device (Controls Inc., Italy). The tested samples were subjected to a uniform loading rate of 50 N/s until fracture. The flexural resistance of samples was calculated using Equation (3):

$$R_f = 1.5 \times \frac{F_f \times l}{b^3} \tag{3}$$

R_f is the flexural strength, in MPa, F_f is the maximum load applied to the prism at the fracture, in N, l is the distance between the support axes (10 mm) and b is the square section of prisms, in mm.

3.2.1 Compressive strength

Following EN 196-1:2016 [35], the compressive strength was performed on the obtained sample halves from flexural tests using a 250-kN hydraulic press machine (Tecnotest, Italy). A displacement-control mechanism at a constant rate of 20 MPa/min was performed. The resistance to compression was calculated using Equation (4):

$$R_c = \frac{F_c}{1600} \tag{4}$$

Where R_c is the compressive strength, in MPa, F_c is the maximum load at fracture, in N, 1600 represents the area of the test samples (i.e., 40×40 mm²).

3.3 Durability assessment

3.3.1 Abrasion resistance measurement

The abrasion resistance test was performed on dry cubic specimens of 71±2 mm after 28 days to determine the surface abrasion loss and the depth of wear using Böhme disc abrader apparatus, as shown in Fig. 6. The measurement protocol was carried out in compliance with the French standard NF EN 14157: 2017 [36].

Prior to testing, the specimens were weighted to an accuracy of ±0.01 g. The samples were clamped into the holder with a load of 294 N (Fig. 6a), and then subjected to 16 abrasion cycles. For each cycle, the disc was rotated by 22 revolutions with a speed of 30 rpm, while 20 g of a standard abrasive powder (Corundum Al_2O_3) was preliminarily poured onto the test track (Fig. 6b). It should be noted that the disc had to be cleaned at the end of each cycle. After 4 cycles, the specimens were gradually turned at 90° to cover all the lateral surfaces. Three specimens were tested for each mix code. The abrasion resistance is calculated as the mean loss in sample volume using the following expression:

$$\Delta V = \frac{m_i - m_f}{\rho_s} \tag{5}$$

ΔV is the loss in volume after 16 cycles, in %, m_i is the initial specimen mass, in g; m_f is the mass of samples after 16 abrasive cycles, in g, ρ_s is the apparent density of the sample, in g/cm^3. Three tests per mix were performed.

3.3.2   Water absorption test

The water absorption test was conducted following the standard practice as in BS 1881–Part 122:2011 [37] on three cubic specimens per mix of size 71±2 mm at the age of 28 days. It should be noted that the water absorption of AFC composites was determined after a total immersion of specimens in water for 24 h using the formula:

$$WA_{24h} = 100 \times \frac{m_w - m_d}{m_d} \tag{6}$$

WA_{24h} is the water absorption coefficient, in %, m_d and m_w stand for the dry and wet mass of the sample before and after immersion, respectively, in kg.
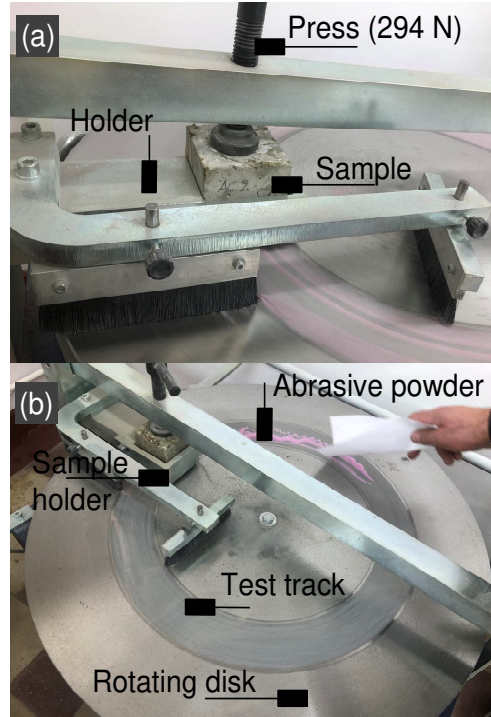
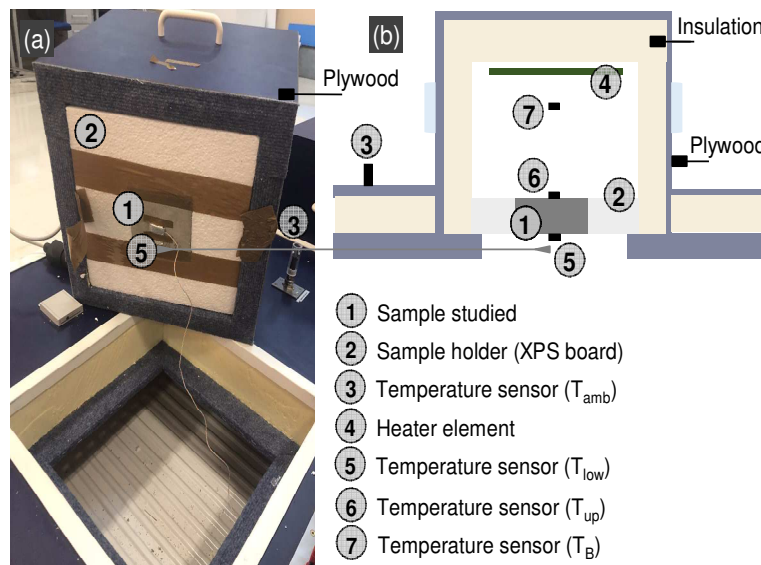**Fig. 6.** Abrasion resistance measurement protocol.

3.4 Hygrothermal properties

3.4.1 Thermal conductivity

The thermal performance of biobased AFC composites was evaluated by characterizing the thermal conductivity in accordance with NF EN ISO 8990 [38]. Measurements were carried out using the *EI702 Cell* apparatus (*DELTALAB-SMT*, France) shown in Fig. 7. The *EI702 Cell* represents the latest version of the two-box method (EI700) used in many research studies over the last decade to establish the effective thermal conductivity of a wide variety of solid materials [9, 17, 39-42]. As shown in Fig.7a, the specimen in question was inserted in an XPS sample holder of surface dimensions of 27x27 cm^2, and placed into the test box. To ensure unidirectional heat transfer through the sample, the upper side was heated by means of an electrical heater (Fig. 6b) while the lower side was air-cooled with a closed-cycle cryostat system. When steady-state equilibrium is achieved, the thermal conductivity value is calculated using Equation (7):

$$\lambda_s = \frac{e_s}{S_s\,(T_{up} - T_{low})_s} \left(\frac{U^2}{R} - \left(\frac{\lambda_{XPS}\,S_{XPS}}{e_{XPS}}\,(T_{up} - T_{low})_{XPS} + C(T_B - T_{amb}) \right) \right) \qquad (7)$$

1   λ_s and λ_{XPS} are respectively the thermal conductivity of the sample and the sample holder, in

2   W/mK, e_s and e_{XPS} represent respectively the thickness of the sample and the sample holder,

3   in m, U is the applied voltage, in V, R is the electrical resistance of the heater element in Ω, T is

4   the temperature of the temperature sensors, shown in Fig 7b, in °C, and C is the heat loss

5   coefficient of the box, in W/°C. A complete discussion of the experimental methodology is

6   detailed in our previous work [39].

1 Sample studied
2 Sample holder (XPS board)
3 Temperature sensor (T_{amb})
4 Heater element
5 Temperature sensor (T_{low})
6 Temperature sensor (T_{up})
7 Temperature sensor (T_B)

7

8   **Fig.7.** Thermal conductivity test box (a) sketch (b).

9   3.4.2   Sorption isotherms

10   Sorption isotherms are one of the main characteristics of materials for the accurate prediction

11   of indoor dynamic conditions in buildings by using coupled heat and mass transfer modeling

12   [43]. Here, AFC's hygroscopic sorption values were determined as stated in the NF EN ISO

13   12571:2021 standard [44] using the climate chamber method to evaluate the ability of

14   produced formulations to transfer water vapor at different successive humidity levels. The

15   experimental protocol consists of maintaining the dry specimens to be tested in temperature-

16   stable environments with different relative humidity plateaus (i.e., under 10, 30, 50, 75 and 90

17   %RH) by means of a climatic chamber (±1 °C and ±5 %RH). For all %RH stages, the chamber's air

18   temperature was kept constant at 23±1 °C. For conditioning, specimens were oven-dried to

19   constant mass at 105±2 °C prior to testing. It is worth mentioning that the drying temperature

1   (i.e., 105 ± 2°C) was selected since no change in the AFC's structure is expected due to the good

2   thermal stability of AF (as given in Fig. 3).

3   During the adsorption test, the specimens were first exposed to 10±5 %RH and weighed

4   periodically at approximately 8h intervals with an accuracy of 0.01 g. The relative humidity

5   gradually increased when all samples' constant mass was observed. As specified in NF EN ISO

6   12570, constant mass was obtained when the difference in mass between three successive

7   weighings separated by at least 24 hours is greater than 0.1%. For the desorption test, the

8   measurement protocol was simply carried out in reverse order to characterize the mass loss

9   profile of the samples as the relative humidity sets decreased. The moisture content mass by

10   mass was measured at steady-state moisture equilibrium from Equation (8):

$$\omega = \frac{m_w - m_d}{m_d} \tag{8}$$

11   ω is the water content of the sample at the moisture equilibrium, in kg/kg, m_w represents the

12   wet mass of the sample, in kg, and m_d is the dry mass of the sample, in kg.

13   3.4.3   Sorption modeling

14   Modeling the sorption behavior of building materials over the entire hygroscopic range using

15   discrete experimental data is of great importance in assessing the dynamic moisture transport

16   in buildings [45]. Numerous theoretical and semi-empirical models have been reported in the

17   literature that better predict the moisture activity of materials in relation to relative humidity

18   [46]. In recently published work on vegetable concrete, particular attention has been paid to

19   GAB (Guggenheim-Anderson-De Boer) model due to its high-fitting accuracy (see e.g. Ref. [23],

20   [47]). The GAB and Handerson models were adopted in this study. The Henderson model was

21   used here for comparison purposes, on the one hand, and for its effectiveness in predicting the

22   water content of porous materials, particularly bio-sourced earth masonry [42], on the other.

23   In GAB model, the moisture content $\omega(\varphi)$ is expressed as a function of relative humidity by

24   Equation (9):

$$\omega_j(\varphi) = \frac{a_j b_j \omega_m \varphi}{(1 - b_j \varphi)(1 + (a_j - 1)b_j \varphi)}, j = ads \ or \ des \tag{9}$$

1 ω_{ads}, ω_{des} ω_m respectively are the main adsorption, desorption isotherms and the monolayer

2 moisture content, in kg/kg, φ is the relative humidity (adim.), both a_j and b_j represent the GAB

3 fitting parameters.

4 For the Henderson model, the sorption isotherm equation is given as follows:

$$\omega_j(\varphi) = \left(-\left(\frac{1}{K_j.T} \right) Ln(1 - \varphi) \right)^{\frac{1}{n_j}}, j = ads \ or \ des \qquad (10)$$

5 ω stand for the adsorption/desorption isotherms, in kg/kg, T represents the reference

6 temperature, equal to 296K. K_j and n_j are the model parameters calculated by fitting

7 experimental data.

8 Note that the model constants (a_j, b_j, ω_m, K_j and n_j) were estimated from the fitting of the

9 experimental data obtained using a non-linear multiple regression analysis based on an

10 Orthogonal Distance Regression (ODR) algorithm. Two statistical metrics were considered to

11 evaluate the prediction accuracy for each model: the sum of squared residuals (SSR) and the

12 coefficient of determination (R^2). These quantitative performance criteria are determined from

13 the following expressions:

$$R^2{}_j = 1 - \frac{\sum_{i=1}^{N} \left(w_{meas,i}\big|_j - w_{esti,i}\big|_j \right)^2}{\sum_{i=1}^{N} \left(w_{meas,i}\big|_j - \overline{w}_{meas,i}\big|_j \right)^2} \qquad (11)$$

$$SSR_j = \sum_{i=1}^{N} \left(w_{meas,i}\big|_j - w_{esti,i}\big|_j \right)^2$$

14 j and i stand respectively for adsorption or desorption test and the ith experimental point, N is

15 the number of experimental data, w_{meas} and w_{esti} are respectively the experimentally

16 measured and estimated equilibrium water contents, in kg/kg, $\overline{w}_{meas,i}$ the mean value of

17 measured equilibrium moisture contents, in kg/kg.

18 3.4.4 Moisture buffer value (MBV)

19 Moisture buffering capacity (MBV) was determined by following the NORDTEST project

20 protocol [48] to assess the ability of AFC formulations to moderate indoor humidity variations

21 in buildings [49]. The MBV test involves sealing the specimens, unlike sorption measurements,

22 as shown in Fig. 8a. Indeed, the samples were sealed with waterproof tape except one surface

to ensure unidirectional moisture transfers (Fig. 8b). Next, the specimens were exposed to daily cyclic relative humidity levels alternating from high (75 %RH) for 8h to low (33%) for 16 h. Before running the %RH cycles, the tested samples were preconditioned in a moist environment at a constant temperature and relative humidity of 23±1°C and 50±5%, respectively, until stabilization. At steady state (i.e., changes in moisture uptake/release were less than 5% between three consecutive cycles), the MBV value of samples is calculated using Equation (12). To ensure the representativeness of the characterized property, both prismatic and cubic samples were used.

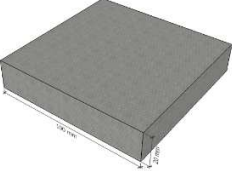$$MBV = 100 \times \frac{\overline{\Delta m}}{A.(RH_{high} - RH_{low})} \tag{12}$$
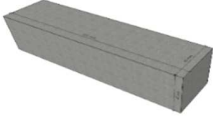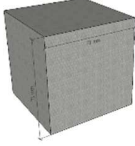
MBV is the moisture buffering value, in g/(m²%RH), $\overline{\Delta m}$ is the moisture content stored or released during the period, in g, A is the open surface area of samples, in m², RH_{high} and RH_{low} are respectively the highest and the lowest values of relativity humidity cycle, in %RH.

Note that %RH cycles were repeated 10 times to ensure that steady-state conditions were obtained. The moisture buffer value of samples was identified as the average of the last three consecutive cycles. Measurements were held at 23 °C, and the chamber's air velocity was maintained as close to 0.1 m/s as possible to simulate typical indoor conditions in buildings. The moisture uptake/release content was quantified by weighting samples outside the climatic chamber three times during uptake and twice during release using an electronic balance with a precision of ±0.01 g.
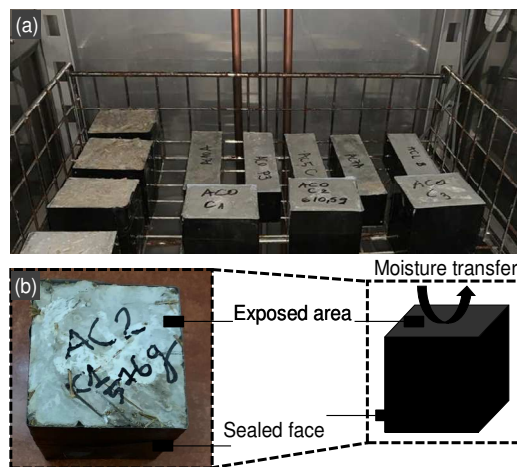
Fig. 8. MBV test (a) climatic chamber (b) sample after sealing.

Table 4. Standard experiments and samples' dimensions adopted in this work.

Specimen	Geometry and dimensions (in mm^3)		Test experiment		
			Objective	Unit/mix	Test protocol
Prismatic		160 × 160 × 40	Flexural strength	3	NF EN 196-1 [35]
			Compressive strength	6	NF EN 196-1 [35]
			Sorption isotherms	3	NF EN ISO 12571 [44]
			MBV test	3	NORDTEST protocol [48]
Cubic		71 × 71 × 71	Apparent density	3	NF EN 12390-7 [33]
			Effective porosity	3	As specified by [34]
			Abrasion	3	NF EN 14157 [36]
			Sorption isotherms	3	NF EN ISO 12571 [44]
			MBV test	3	NORDTEST protocol [48]
			Water absorption	3	BS 1881-122 [37]
Slab		100 × 100 × 20	Thermal conductivity	3	NF EN ISO 8990 [38]
Tests performed on crushed samples (raw materials)					
-	-	-	True density	3	NF EN ISO 1183-1 [28]

4 Results and discussion

4.1 Physical and mechanical properties of AFC formulations

The AFC formulations' apparent density, effective porosity, uniaxial and flexural tests at 28 days of age are depicted in Table 5. Each reported value is written as the mean of three measures ± the standard deviation (mean±s.d.). In contrast, compressive strength values stand for the average obtained by testing each mix's six halves (resulting from the flexural test).

The results show that the density of AFC mixtures decreased with increasing AF content. This is expected since the incorporation of plant fibers increases the number of voids in the cement matrix, which is also confirmed by the obtained effective porosity values. The same behavior is always verified for plant-based LWC concrete [1]. Furthermore, liquid pycnometer tests (see Table 2) show that Alfa fibers exhibit a low true density of 1.25 g/cm^3 compared to the cement matrix (ρ_{true}=2.27 g/cm^3), which explicitly explains the latter finding. By comparing AFC10 and AFC0 formulations, it was found that 10wt% AF decreased the density by 20.4%, resulting in an almost 30% increase in porosity.

Similarly, the compressive and flexural strength values presented in Table 5 show that both characteristics decreased with increasing AF content. For 5wt% AF, the compressive and

flexural strengths dropped by 80.2% and 60.6%, respectively. This result is in line with the recent study conducted by Sakami et al. [17] on AF mortar composites, who observed a compressive resistance reduction of 82.5% at the same weight addition rate. However, unlike AFC2, they found no discernible difference in flexural strength when adding 2wt% AF, which is ascribed to the use of AF with a tiny diameter ranging from 0.7–1 mm that provides better fiber-matrix adhesion [50]. For the same fiber length and mix design, Benmansour et al. [1] reported a drastic decrease in compressive resistance (92%) with 5wt% date palm fibers (DPF) inclusion. This validates the hypothesis of incorporating AF as reinforcing elements in LWC composites. This is why, despite the significant reduction in mechanical strengths, an intriguing feature was noticed when evaluating the response of tested AFC composites following ultimate failures (i.e., Fig. 9).

Table 5. Physical and mechanical characteristics of tested AFC mixes (mean±s.d.).

| Mix code	Physical properties		Mechanical properties (at 28 days)	
	Dry density	Effective porosity	Compressive strength	Flexural strength
	Kg/m^3	%	MPa	
AFC0	1682±06	29.3±2.3	19.14±1.19	4.16±0.16
AFC2	1587±08	34.0±3.1	11.90±1.02	1.83±0.04
AFC5	1537±16	34.2±0.9	03.78±0.62	1.64±0.50
AFC7	1406±10	41.0±2.8	01.28±0.04	0.59±0.03
AFC10	1338±07	41.8±1.6	00.66±0.06	0.54±0.03

Fig. 9. Photographs of specimens after (a) flexural and (b) compressive strength tests. The flexural cracks of AFC0 and AFC5 specimens depicted in Fig. 9a clearly reveal that samples without AF (AFC0) were split into two halves. At the same time, AF-based formulations (e.g., AFC5) remained consistent with a single crack closer to the sample's mid-span. This proves evidence that AF can serve as a natural reinforcement aggregate for a cement matrix. Moreover, it is also evident from the obtained compressive crack patterns formed in the specimens and shown in Fig.9b that AF inclusion in bio-concrete resulted in a more consolidated structure due to the improved fiber/matrix bonds. The reinforcing character of AF was recently reported in [17], which showed that 1wt% AF increases the compressive and flexural strengths of LWC concrete by 9% and 10.45%, respectively. Existing studies on plant-based building materials have found similar results regarding the efficiency of plant fibers in preventing matrix separation at ultimate fracture (e.g., [51], [52]). Furthermore, for works related to fiber-reinforced concrete, Zhang et al. [53] also reported similar conclusions when integrating short AR-glass fibers into a cementitious matrix, indicating that AF may be competitive with synthetic fibers for designing bio-based reinforced concrete. More in-depth building-scale investigations are required to evaluate the use of plant fibers in designing lightweight concretes with enhanced seismic resistance

4.2 Thermal conductivity of AFC formulations

Fig. 10 depicts the thermal conductivity of prepared AFC formulations as a function of density. It compares the obtained values to those reported in some studies conducted on bio-based concrete (i.e., [1] and [54]). As in the literature, the results show a reduction in the thermal conductivity of concrete with increasing AF. Besides the AF's low thermal conductivity (~0.042 W/mK [55]), the decrease is explained by the fact that AF inclusion reduces the cementitious mixes' density, leading to greater microstructural porosity (see Table 5). In addition, the incorporation ratios and the thermal insulation of bio-concrete were found to have a very clear relationship as shown in Fig. 8a. Generally, the higher the amount of fiber, the lower the thermal conductivity. Moreover, it was noticed that above around 1400 kg/m^3, the thermal conductivity decreases linearly (see dotted lines in Fig. 10b), and below this density, the variation has an exponential trend [54], showing the negligible effect of bio-based aggregates in

reducing the thermal conductivity of low-density materials. A similar finding can also be made by examining the study conducted by Benmansour et al. [1] who investigated the influence of date palm fibers on the thermomechanical performance of bio-concrete using different fiber lengths, highlighting the effectiveness of short fibers (approximately 3 cm length) in reducing the thermal conductivity of cement-based concrete.

Indeed, the present study shows that the addition of 10wt% of 3 cm length AF reduced the thermal conductivity of AFC mixes from 0.591 to 0.193 W/mK, representing an improvement of 67% in the thermal insulation. It is worth mentioning that Benmansour et al. [1] revealed that bio-concrete incorporating the same weight rate (i.e., 10wt%) of date palm reduced the thermal conductivity by 73%. This difference can be attributed to the initial density of raw materials and the compaction process. For the same cement matric, however, Alfa fibers may be more effective due to their rigid nature of AF which provides more intra-and extra fiber/matrix voids.
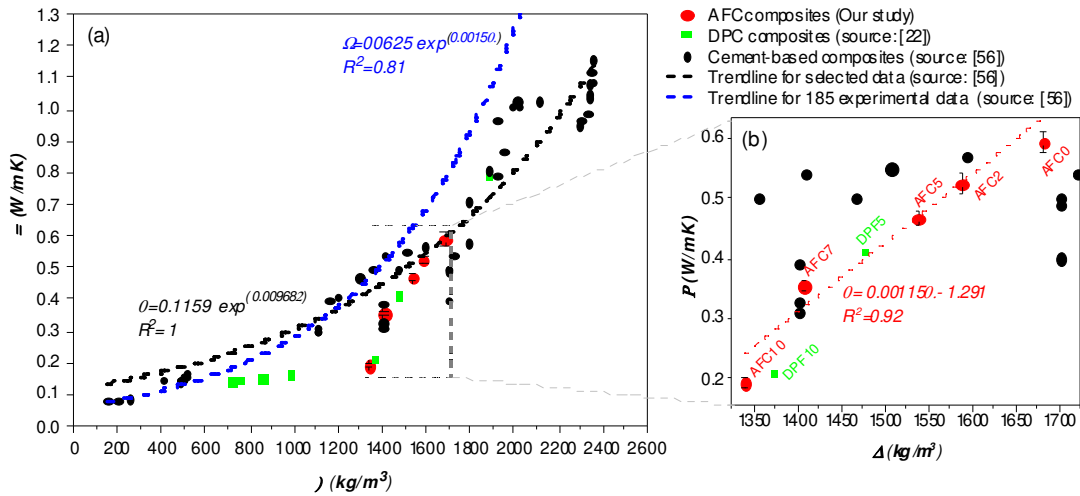
Fig. 10. Thermal conductivity of AFC formulations vs. data reported in the literature (a) enlargement (b).

4.3 The durability of AFC formulations

The average water absorption and abrasion volume loss of the AFC mixtures as a function of fiber content are presented in Fig. 11. The results show that AFC2 and AFC5 formulations exhibit lower mass loss following the abrasion test than AFC0 without AF addition, accounting for abrasion resistance and an improvement in abrasion resistance of 35.4% and 34%,

respectively. Above 5wt%, the AF addition negatively affected the fiber-cement cohesion, with a maximum volume loss of up to 43.8% when 10wt% AF was incorporated. It is evident from observing the wear surfaces of tested samples shown in Fig. 12a that, from 7wt% of AF content onwards, the AFC mixtures have begun to lose the binding characteristics of cement, which is clearly noticed by the high mass loss and cracks formed after the abrasion test of AFC7 side faces. This implies that 0–5wt% incorporation range is suitable for improving concrete abrasion resistance. In addition to the increased durability, the wear surface pattern of the AFC5 specimen displayed in Fig. 12b indicates that integrating AF into the cement matrix generates macro-pores responsible for thermal insulation enhancements.

Indeed, the addition of supplementary materials such as pozzolanic (e.g., fly ash [56]) and synthetic fibrous materials (e.g., steel fibers, glass fibers and polypropylene fibers [57]) have been reported in the literature as active components to enhance the abrasion resistance of concrete. Regrading plant-based fibers, we are aware of only one recent paper that has looked into the influence of coir fibers on the abrasion resistance of cement-based concrete (i.e., Ref. [58]). The study demonstrated the negative effect of coir fibers on abrasion and compressive strength, mainly attributed to the plant fiber lumps in the matrix. In the present paper, however, the inclusion of short AF (< 5wt%) in concrete have shown similar tendency effects to that of polypropylene (PP) fibers (< 1vol%) on reducing the wear depth and improving the abrasion resistance [59], which validated the reinforcing character of AF. Furthermore, Ajouguim et al. [60] have stated that AF fibers can even be used to obtain cost-effective and eco-efficient concrete with improved mechanical properties compared to concrete reinforced with PP fibers. Consequently, AF fibers can be a promising green alternative to synthetic fibers for improving the durability of bio-LWC concrete.
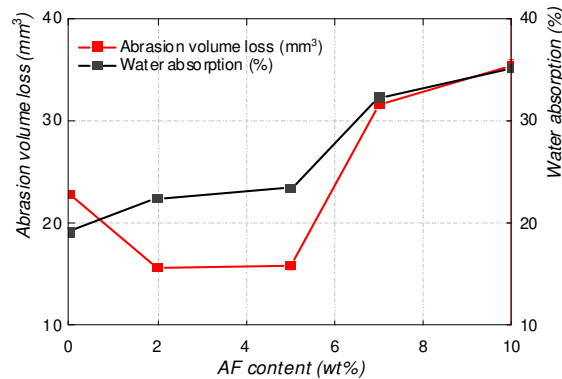
Fig. 11. Abrasion volume loss and water absorption of AFC composites.

With respect to water absorption, the results revealed, as expected, that AF reinforced concrete mixtures exhibit higher water absorption when compared to concrete without any AF. Fig. 11 also shows that water absorption increased with increasing AF content. This is owing to two principal reasons : (i) the hydrophilic characteristic of plant fibers and (ii) the voids created in the cement matrix by AF. Similar conclusions were reported in other studies (e.g., [60]), emphasizing the importance of fiber treatment to enhance the water-penetration resistance of vegetable concrete.
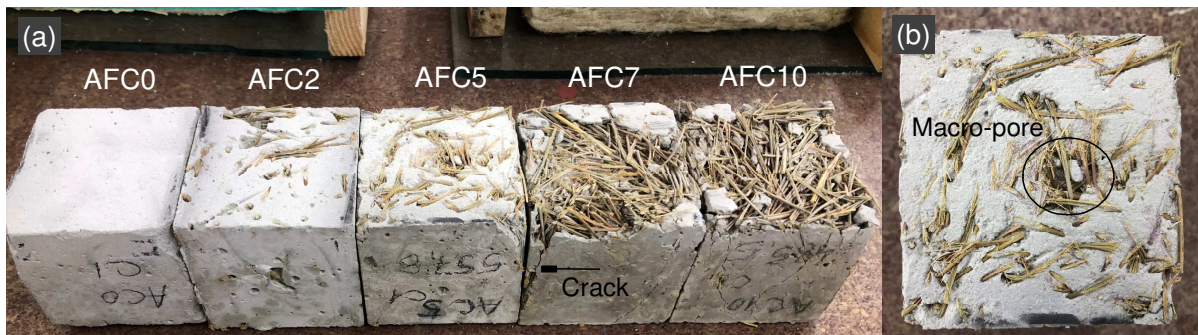
Fig. 12. Photographs of abraded surfaces of (a) AFC specimens (b) AFC5.

4.4 Thermomechanical performance and optimum AFC mixes

Thermal conductivity and compressive strength are the main material selection criteria that must be considered in the design of thermal insulating and load-bearing structures. For this reason, it would be useful to identify the appropriate AFC formulations for use in both building applications. Fig. 13 depicts the evolution of the thermal conductivity and compressive strength values of AFC mixtures as a function of density.

23

For the purpose of classification and comparison with plant-based concretes developed in the literature such as date palm concrete [1] and others (e.g., [7], [61]), the well-known RILEM functional classification of lightweight concrete [22] was adopted. This functional classification purposes to classify LWC into two main classes (i.e., class I, II and III) based on the displayed minimum thermomechanical requirements given in Fig. 13. Note that Class–I grade concrete characterises structural concretes meeting the thermomechanical threshold pair (λ=0.75 W/mK; R_c=15 MPa).

Many works aimed at classifying vegetable concrete mixtures according to their appropriate applications using the RILEM classification [1], [7], [61], [62]. For instance, Benmansour et al. [1] developed the same concrete mix with 15 wt% date palm fibers (DPF) for structural applications. Boumhaout et al. [62] also attempted to develop date palm concrete mixtures for insulating and structural uses based on a mass mix design of 3:4 sand and 1:4 cement. They found that incorporating 48vol% DPF can be used for designing structural and insulating LWC with a compressive strength of ∼4 MPa. More recently, Ahmad et al. [7] have developed vegetable geopolymer-based concrete incorporating 33% of corn stalks for insulating and structural purposes with a compressive strength value of 3.59 MPa.

In the present study, the classification patterns in Fig. 13 clearly show that AFC2 and AFC5 mixtures meet the requirements for class-II grade concrete; i.e., they can be used as structural and insulating building materials, whereas the AFC10 formulation is classified as a class-III grade concrete that can only be used for thermal insulating purposes. AFC7 mix design does not satisfy both types of technical requirements, according to RILEM classification. As they provide the best thermal insulation quality and acceptable mechanical performances, AFC5 (R_c=3.78 MPa) and AFC10 (λ=0.19 W/mK) are the optimal formulations to be considered for structural and insulation purposes, respectively.

$$R_c = 9E\text{-}7e^{0.0101\rho}$$
$$R^2 = 0.99$$

RILEM Classification of lightweight concrete:

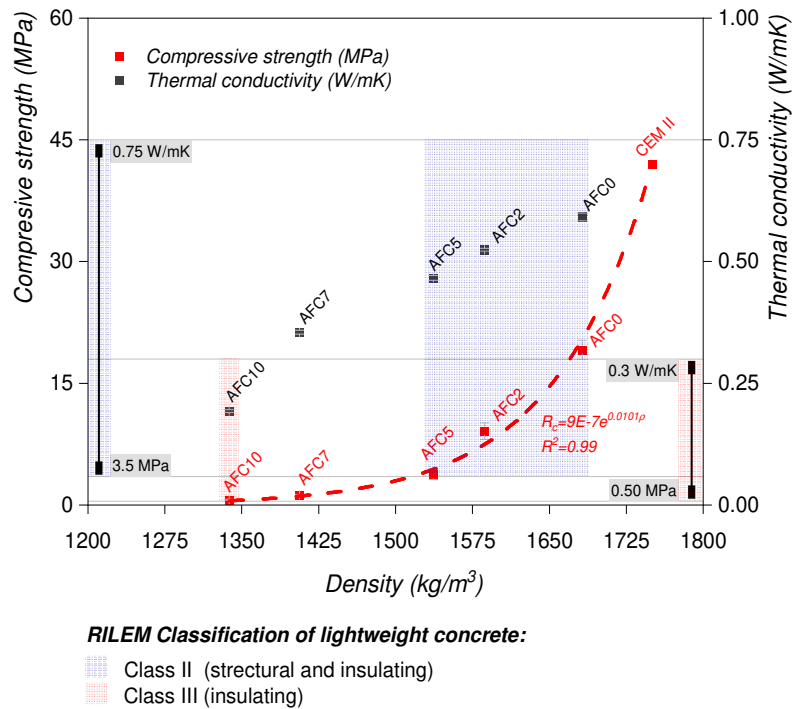Class II (strectural and insulating)
Class III (insulating)

Fig. 13. Thermo-mechanical performance of AFC concrete.

In what follows, the focus will be on the hygric properties of the selected mixes. The sorption isotherms of the AFC0 formulation are also considered to investigate the impact of AF addition on the hygric performance of lightweight vegetable concrete.

4.5 Sorption isotherms of optimal AFC formulations

Fig. 14 gives the adsorption/desorption isotherms of AFC0, AFC5 and AFC10 formulations at 23°C. Each experimental data stands for the average evaluated on three specimens of the same mix. Evident changes between the different formulations were observed. Indeed, cement-based composites filled with AF exhibit higher adsorption capacities (Fig. 13a) than specimens without AF over the studied relative humidity range. In addition, the moisture uptake of mixtures significantly increases with increasing AF contents. For example, at %RH equal to 90%, the moisture content of AF-free samples (AFC0) was ω=0.045 kg/kg, whereas it showed a significant increase to 0.061 kg/kg and 0.075 kg/kg for AFC5 and AFC10 mixes, respectively. These results demonstrated that AF inclusion increases the moisture storage capacity of cement-based concrete, which is attributed to the high porosity and absorption capacity of plant aggregates, as previously reported by [63], [64].

25

The estimated fitting constants for each model are listed in Table 5. The adjustment curves using the GAB (solid lines) and Henderson (dotted lines) models for the three selected formulations are also displayed in Fig. 13(a)-(c). For all cases, a convergence tolerance value of 1E-9 was achieved. It was clearly noticed that the adsorption/desorption isotherms of all AFC specimens followed a similar sigmoidal pattern (Fig. 13a) which corresponds to type-II adsorption isotherms according to the IUPAC classification. As a result, AFC mixtures are considered macro-porous materials with high adsorption energy and broad pore size distribution [65], [66].

By observing Table 6, it can be seen that both models provide an excellent fit to the obtained experimental data with a minimum correlation coefficient above 0.999. However, concerning the sum of squared residuals (SSR) values obtained, the GAB model shows a better performance in describing the adsorption behavior of AFC formulations with a maximum SSR of about $0.858 \cdot 10^{-5}$, compared to the Handerson model which gives a maximum SSR of $6.822 \cdot 10^{-5}$. This is attributed to the high performance of the GAB model in predicting the adsorption behavior of AFC composites at a low %RH range, as shown in Fig. 13a. For plant aggregate-free specimens (i.e., AFC0), the GAB model consistently provided the most accurate predictions for the desorption process (Fig. 13b) with an SSR of $0.848 \cdot 10^{-5}$. On the other hand, the Henderson model better described the desorption behavior of bio-based formulations. As a result, the GAB model is more suitable for describing the sorption isotherms of non-bio concrete. In contrast, the Henderson model is the most appropriate for the sorption modeling of composite building materials. This conclusion was previously noted by Saidi et al. [67], who used several sorption models to evaluate the sorption-desorption behavior of stabilized and unstabilized earth construction materials.

Finally, the complete sorption-desorption isotherms of studied formulations are given in Fig. 14c, showing the high sorption capacities of AF-based concretes, which could effectively moderate the relative humidity fluctuations and improve the indoor thermal comfort level in buildings [68].
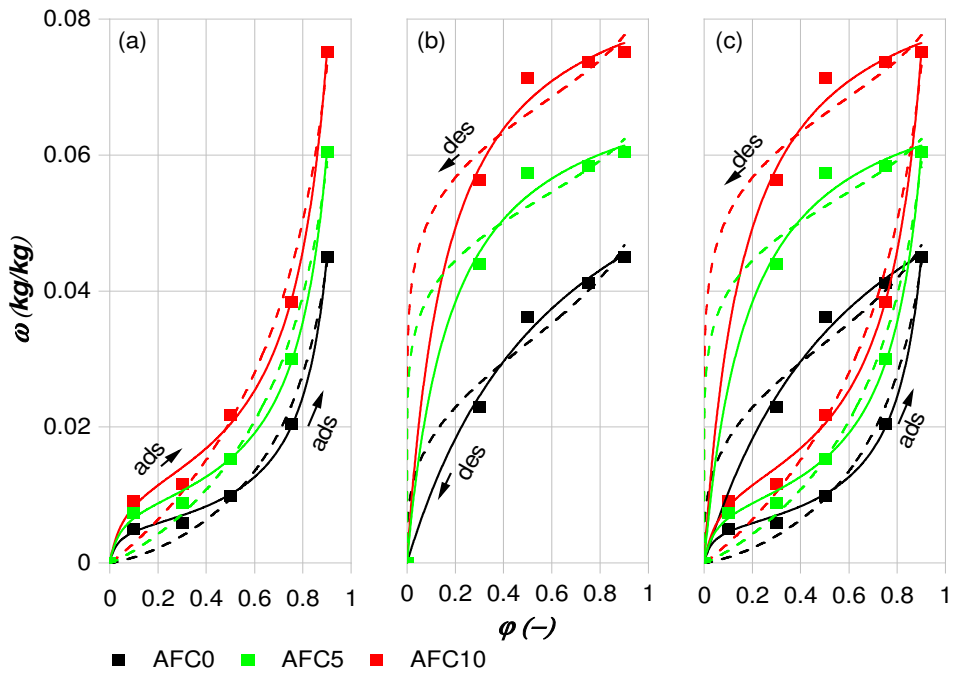
Fig. 14. Comparison of experimental (a) adsorption (b) desorption and (c) all sorption isotherms for AFC0, AFC5 and AFC10. Experimental data (separate dotes) and fitting curves using GAB (solid lines) and Henderson model (dashed lines).

1 **Table 6.** Fitting results of sorption isotherms of selected AFC formulations.

Adsorption				
Model	Parameters	Specimens		
		AFC0	AFC5	AFC10
GAB	w_m	0.00532	0.00837	0.01148
	C	31.32122	23.14732	18.04659
	K	0.98089	0.95893	0.94346
	R^2	1	1	0.99999
	$SSR\ (\times 10^{-5})$	0.194	0.409	0.858
Henderson	C	26.30466	28.42163	28.51103
	n	0.78019	0.88792	0.96148
	R^2	0.99998	0.99996	0.99994
	$SSR\ (\times 10^{-5})$	2.882	4.69	6.822
Desorption				
GAB	w_m	0.07881	0.07413	0.09089
	C	3.95482E4	2.52151E5	2.33019E5
	K	3.81127E-5	2.12587E-5	2.53682E-5
	R^2	0.99999	0.99998	0.99997
	$SSR\ (\times 10^{-5})$	0.848	143.2	431.9
Henderson	C	5.15883E4	4.85304E8	3.90755E8
	n	3.27036	6.9085	7.41597
	R^2	0.99997	0.99996	0.99995
	$SSR\ (\times 10^{-5})$	3.069	4.152	5.135

2 4.6 Buffering capacity of optimal AFC formulations

3 The average MBV value on three specimens for AFC5 and AFC10 as well as some values

4 reported by other works on biosourced concrete are presented in Fig. 15. The experimental

5 results show that incorporating AF fibers increases the moisture buffering capacity of cement-

6 based concrete. Moisture buffering capacities of 2.29 g/(m2%RH) and 3.13 g/(m2%RH) were

7 achieved when adding 5wt% and 10wt% AF, respectively, allowing the designed AFC

8 formulations to be classified as EXCELLENT moisture regulators according to NORDTEST

9 classification [48]. This finding is in good agreement with the previous study conducted by

10 Belakroum et al. [69] who found that the MBV value of concrete increases with increasing plant

11 fiber content.

12 Moreover, one interesting observation from Fig. 15 is that cement-based concrete has higher

13 MBV values than lime-based concretes. For instance, Belakroum et al. [69] used 35wt% date

14 palm fibers to develop a biosourced lime-based concrete mixture with an MBV value of 3.1

15 g/(m2%RH). Channouf et al. [23] achieved an excellent moisture buffer value around 2.97

g/(m2%RH) by incorporating 15wt% DPF in a cement-based concrete. The reported values are consistent with the range of our experimental data, particularly those found in [23], which is explained by the fact that developed plant-based concretes were prepared using the same methodology as in the present work. Consequently, it can be concluded that Alfa fibers represent promising plant-based aggregates for developing lightweight vegetable concretes with enhanced hygric properties for energy-efficient buildings.
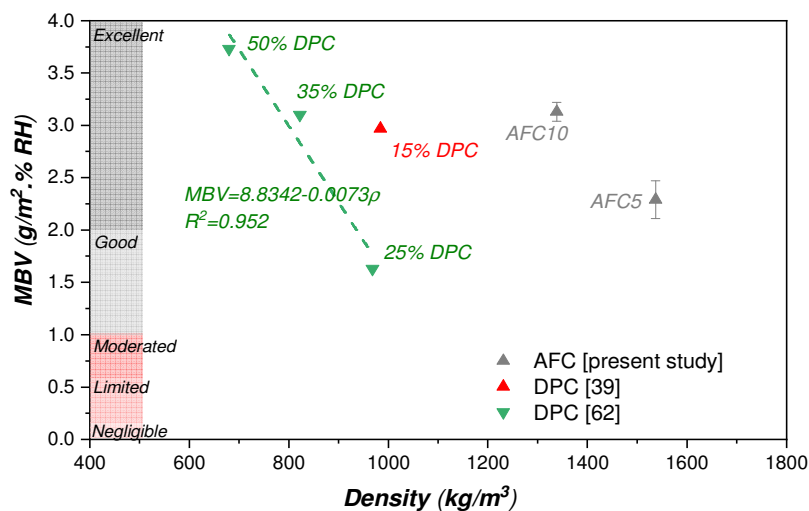
Fig. 15. MBV values of selected AFC formulations.

5 Conclusion

This work purposes of studying the potential use of short Alfa fibers (AF) as plant-based aggregates for developing lightweight vegetable concrete with improved hygrothermal characteristics. In order to identify optimum incorporation rates for the design of structural and thermally insulating building elements, five cement-based formulations made with different AF weight contents (i.e., 0, 2, 5, 7 and 10wt%) were developed and experimentally characterized. Based on the conducted experiments, the following main conclusions were pointed out:

- Increasing AF content considerably improves the thermal insulation quality of cement-based concrete while lowering compressive and flexural strengths, e.g., the addition of 10wt% FA reduces the thermal conductivity, compressive and flexural strengths by 67%, 80.2% and 60.6%, respectively.

- By adding short AF into the cement matrix, the abrasion resistance of AFC formulations was improved. the AF inclusion in the range 2–5wt% resulted in a significant improvement of the abrasion resistance by 34–35.4%. Above 5wt% AF content, the AFC mixtures lose their abrasion resistance compared to the control mix (i.e., AFC0).
- According to the RILEM functional classification of lightweight concrete, vegetable concrete filled with 5wt% AF is classified as class-II grade concrete, which can be used as structural and thermal insulating materials. At the same time, formulations containing 10wt% AF are only suitable as thermal insulating and filling materials.
- The integration of AF significantly increases the sorption capacities and the moisture buffering of cement-based concrete; e.g., adding 5wt% and 10wt% of AF can be used for the production of vegetable concrete with excellent moisture buffering value around 2.29 $g/(m^2\%RH)$ and 3.13 $g/(m^2\%RH)$, respectively.
- By virtue of this study, it can be concluded that Alfa fibers present promising agro-aggregates for designing energy-efficient composites. Adopting 5–10wt% AF in concrete production would result in green building materials suitable for eco-construction and "thermal comfort enhancement in buildings.

Conflict of interest

The authors declare that there is no conflict of interest regarding the publication of this paper.

References

[1]N. Benmansour, A. Agoudjil, A. Gherabli, A. Kareche, A. Boudenne, Thermal and mechanical performance of natural mortar reinforced with date palm fibers for use as insulating materials in building, Energy Build., 81 (2014), pp. 98-104. 10.1016/j.enbuild.2014.05.032.

[2] A. Bahurudeen, D. Kanraj, V. Gokul Dev, M. Santhanam. Performance evaluation of sugarcane bagasse ash blended cement in concrete. Cem. Concr. Compos., 59 (2015), pp. 77-88. 10.1016/j.cemconcomp.2015.03.004.

[3] A.K. Tedjditi, F. Ghomari, O. Taleb, R. Belarbi, R.T. Bouhraoua, Potential of using virgin cork as aggregates in development of new lightweight concrete, Constr. Build. Mater., 265 (2020) 120734. 10.1016/j.conbuildmat.2020.120734.

[4] M.U. Farooqi, M. Ali, Contribution of plant fibers in improving the behavior and capacity of reinforced concrete for structural applications, Constr. Build. Mater., 182 (2018) 94-107.

[5] T. Lecompte, Matériaux bio-sourcés pour le bâtiment et stockage temporaire de carbone, Technique de l'ingénieur. (2019).

[6] M. Boutin, C. Flamin, S. Quinton, G. Gosse, Analyse du cycle de vie: Compounds thermoplastiques chargés fibres de chanvre et Mur en béton de chanvre banché sur ossature bois, Rapport d'Étude INRA Lille, Réf. MAP 4 (2005).

[7]] M.R. Ahmad, B. Chen, M.A. Haque, S.Y. Oderji, Multiproperty characterization of cleaner and energy-efficient vegetal concrete based on one-part geopolymer binder. J. Clean. Prod., 253 (2020) 119916, 10.1016/j.jclepro.2019.119916.

[8] J.P. Holman. Heat Transfer (Si Units) Sie. Tata McGraw-Hill Education (2008).

[9] M. Charai, H. Sghiouri, A. Mezrhab, M. Karkri, Thermal insulation potential of non-industrial hemp (Moroccan cannabis sativa L.) fibers for green plaster-based building materials. J. Clean. Prod., 292 (2021) 126064, 10.1016/j.jclepro.2021.126064.

[10] Y. Shang, F. Tariku, Hempcrete building performance in mild and cold climates: Integrated analysis of carbon footprint, energy, and indoor thermal and moisture buffering, Build. Environ., 206 (2021) 108377, 10.1016/j.buildenv.2021.108377.

[11] M. Mehravar, A. Veshkini, S. Veiseh, R. Fayaz, Physical Properties of Straw Bale and its Effect on Building Energy Conservation and Carbon Emissions in Different Climatic Regions of Iran, Energy Build., (2021) 111559, 10.1016/j.enbuild.2021.111559.

[12] P. Strandberg-de Bruijn, A. Donarelli, K. Balksten, Full-scale studies of improving energy performance by renovating historic Swedish timber buildings with hemp-lime, Appl. Sci., 9(12) (2019) 2484, 10.3390/app9122484.

[13] A.D. Tran Le, C. Maalouf, T.H. Mai, E. Wurtz, F. Collet, Transient hygrothermal behaviour of a hemp concrete building envelope, Energy Build., 42 (2010), pp. 1797-1806, 10.1016/j.enbuild.2010.05.016.

[14] P. Aversa, A. Marzo, C. Tripepi, S. Sabbadini, G. Dotelli, P. Lauriola, C. Moletti, V. Luprano, Hemp-lime buildings: thermo-hygrometric behaviour of two case studies in North and South Italy, Energy Build., 247 (2021) 111147, 10.1016/j.enbuild.2021.111147.

[15] A. Shea, M. Lawrence, P. Walker, Hygrothermal performance of an experimental hemp–lime building, Constr. Build. Mater., 36 (2012) 270-275, 10.1016/j.conbuildmat.2012.04.123.

[16] B. Moujalled, Y. Aït Ouméziane, S. Moissette, M. Bart, C. Lanos, D. Samri, Experimental and numerical evaluation of the hygrothermal performance of a hemp lime concrete building: a long term case study, Build. Environ., 136 (2018), pp. 11-27, 10.1016/j.buildenv.2018.03.025.

[17] S. Sakami, L. Boukhattem, M. Boumhaout, B. Benhamou, Development of Alfa Fiber-Based Mortar with Improved Thermo-Mechanical Properties, Appl. Sci., 10(22) (2020) 8021, 10.3390/app10228021.

[18] Y. Cherradi, I.C. Rosca, C. Cerbu, H. Kebir, A. Guendouz, M. Benyoucef, Acoustic properties for composite materials based on alfa and wood fibers, Appl. Acoust., 174 (2021) 107759, 10.1016/j.apacoust.2020.107759.

[19] M. Khelifa, N. Leklou, T. Bellal, R. Hebert, B. Ledesert, Is alfa a vegetal fiber suitable for making green reinforced structure concrete?, Eur. J. Environ. Civil Eng., 22 (6) (2018), pp. 686-706, 10.1080/19648189.2016.1217792.

[20] S. Ajouguim, J. Page, C. Djelal, M. Waqif, L. Saâdi, Impact of Alfa fibers morphology on hydration kinetics and mechanical properties of cement mortars, Constr. Build. Mater., 293 (2021) 123514, 10.1016/j.conbuildmat.2021.123514.

[21] M.-R. Khelifa, S. Ziane, S. Mezhoud, C. Ledesert, R. Hebert, B. Ledesert, Compared Environmental Impact Analysis of Alfa and Polypropylene Fibre-Reinforced Concrete, Iran. J Sci. Technol. Trans. Civ. Eng., 45 (2021), pp. 1511–1522, 10.1007/s40996-020-00555-x.

[22] L. Rilem, Functional classification of lightweight concrete, Mater. Struct 11 (1978) 281-283.

[23] N. Chennouf, B. Agoudjil, A. Boudenne, K. Benzarti, F. Bouras, Hygrothermal characterization of a new bio-based construction material: Concrete reinforced with date palm fibers, Constr. Build. Mater., 192 (2018), pp. 348-356, 10.1016/j.conbuildmat.2018.10.089.

[24] NF EN 197-1 (2012), Cement - Part 1: composition, specifications and conformity criteria for common cements.

[25] NF EN 1015-1 (1999), Methods of test for mortar for masonry. Part 1: determination of particle size distribution (by sieve analysis).

[26] S. Ajouguim, K. Abdelouahdi, M. Waqif, M. Stefanidou, L. Saâdi, Modifications of Alfa fibers by alkali and hydrothermal treatment, Cellulose, 26 (2019), pp. 1503-1516, 10.1007/s10570-018-2181-9.

[27] F.E. El-Abbassi, M. Assarar, R. Ayad, A. Bourmaud, C. Baley, A review on alfa fibre (Stipa tenacissima L.): From the plant architecture to the reinforcement of polymer composites, Compos. Part. A Appl. Sci. Manuf., 128 (2020), p. 105677, 10.1016/j.compositesa.2019.105677.

[28] NF EN ISO 1183-1 (2019), Plastics - Methods for determining the density of non-cellular plastics - Part 1 : immersion method, liquid pycnometer method and titration method.

[29] M. El Achaby, Z. Kassab, A. Barakat, A. Aboulkas, Alfa fibers as viable sustainable source for cellulose nanocrystals extraction: Application for improving the tensile properties of biopolymer nanocomposite films, Ind. Crops Prod., 112 (2018), pp. 499-510, 10.1016/j.indcrop.2017.12.049.

[30] L. Segal, J.J. Creely, A.E. Martin, C.M. Conrad, An empirical method for estimating the degree of crystallinity of native cellulose using the X-ray diffractometer, Text. Res. J., 29 (1959), pp. 786-794.

[31] A. Benyahia, A. Redjem, Z.E.A. Rahmouni, A. Merrouche, Study of the mechanical properties of a composite material: Alfa fibers/unsaturated polyester, Rom. J Mater., 46(1), pp. 25–33.

[32] N.B.R. Legrand, M. Lucien, O. Pierre, B.E. Fabien, N.P. Marcel, A.A. Jean, Physico-chemical and thermal characterization of a lignocellulosic fiber, extracted from the bast of Cola lepidota stem, J. Miner. Mater. Charact. Eng., 08 (2020), pp. 377-392, 10.4236/jmmce.2020.85024.

[33] NF EN 12390-7 (2019), Testing hardened concrete - Part 7 : density of hardened concrete.

[34] C. Lian, Y. Zhuge, S. Beecham, The relationship between porosity and strength for porous concrete, Constr. Build. Mater., 25 (2011), pp. 4294-4298, 10.1016/j.conbuildmat.2011.05.005.

[35] NF EN 196-1 (2016), Methods of testing cement - Part 1 : determination of strength.

[36] NF EN 14157 (2017), Natural stone test methods - Determination of the abrasion resistance.

[37] BS 1881-122 (2011), Testing concrete - Method for determination of water absorption.

[38] NF EN ISO 8990 (1996), Thermal insulation. Determination of steady-state thermal transmission properties. Calibrated and guarded hot box.

[39] M. Charai, H. Sghiouri, A. Mezrhab, M. Karkri, New methodology for measuring the thermal conductivity of small samples using the boxes method with reduced sensors, Int. J Thermophys. 41 (2020), 10.1007/s10765-020-02649-0.

[40] R. Alyousef, O. Benjeddou, C. Soussi, M.A. Khadimallah, M. Jedidi, Experimental study of new insulation lightweight concrete block floor based on perlite aggregate, natural sand, and sand obtained from marble waste, Adv. Mater. Sci. Eng., 2019 (2019), p.14, 10.1155/2019/8160461.

[41] H. Lakrafli, S. Tahiri, A. Albizane, M. Bouhria, M. El Otmani, Experimental study of thermal conductivity of leather and carpentry wastes, Constr. Build. Mater., 48 (2013), pp. 566-574, 10.1016/j.conbuildmat.2013.07.048.

[42] M. Charai, A. Mezrhab, L. Moga, A structural wall incorporating biosourced earth for summer thermal comfort improvement: Hygrothermal characterization and building simulation using calibrated PMV-PPD model, Build. Environ. (2022) 108842, 10.1016/j.buildenv.2022.108842.

[43] M. Rahim, O. Douzane, G. Promis, T. Langlet, Numerical investigation of the effect of non-isotherm sorption characteristics on hygrothermal behavior of two bio-based building walls, Build. Eng., 7 (2016), pp. 263-272, 10.1016/j.jobe.2016.07.003.

[44] NF EN ISO 12571 (2021) Hygrothermal performance of building materials and products - Determination of hygroscopic sorption properties.

[45] J. Delgado, E. Barreira, N.M. Ramos, V.P. De Freitas, Hygrothermal numerical simulation tools applied to building physics, Springer Science & Business Media (2012).

[46] M. Mozaffari Majd, V. Kordzadeh-Kermani, V. Ghalandari, A. Askari, M. Sillanp, Adsorption isotherm models: a comprehensive and systematic review (2010-2020), Sci. Total Environ. (2021), p. 151334, 10.1016/j.scitotenv.2021.151334.

[47] M.R. Ahmad, B. Chen, Influence of type of binder and size of plant aggregate on the hygrothermal properties of bio-concrete, Constr. Build. Mater., 251 (2020) 118981, 10.1016/j.conbuildmat.2020.118981.

[48] C. Rode, R. Peuhkuri, H. Lone, B. Time, A. Gustavsen, T. Ojanen, J. Ahonen, K. Svennberg, Moisture buffering of building materials, Nordic Innovation Centre Report: BYG-DTU R-126, ISSN, 2005, pp. 1601–2917.

[49] A.D. Tran Le, J.S. Zhang, Z. Liu, D. Samri, T. Langlet, Modeling the similarity and the potential of toluene and moisture buffering capacities of hemp concrete on IAQ and thermal comfort, Build. Environ., 188 (2021) 107455, 10.1016/j.buildenv.2020.107455.

[50] A. Kriker, G. Debicki, A. Bali, M. Khenfer, M. Chabannet, Mechanical properties of date palm fibres and concrete reinforced with date palm fibres in hot dry climates, Cem. Concr. Compos., 27 (2005), pp. 554-648.

[51] M. Charai, M. Salhi, O. Horma, A. Mezrhab, M. Karkri, S. Amraqui, Thermal and mechanical characterization of adobes bio-sourced with Pennisetum setaceum fibers and an application for modern buildings, Constr. Build. Mater., 326 (2022) 126809, 10.1016/j.conbuildmat.2022.126809.

[52] M.S. Islam, K. Iwashita, Earthquake resistance of adobe reinforced by low cost traditional materials, J Natural Disaster Sci., 32 (1) (2010), pp. 1-21.

[53] Q. Zhang, S. Li, S. Gong, G. Zhang, G. Xi, Y. Wu, Study on Flexural Properties of Basalt Fiber Textile Reinforced Concrete (BTRC) Sheets Including Short AR-Glass Fibers, Front. Mater., 7 (2020), 10.3389/fmats.2020.00277.

[54] I. Asadi, P. Shafigh, Z.F. Bin Abu Hassan, N.B. Mahyuddin, Thermal conductivity of concrete – A review, J. Build. Eng., Nov., 20 (2018), pp. 81-93.

[55] M. Dallel Evaluation du potentiel textile des fibres d'Alfa (Stipa Tenacissima L.): Caractérisation physico-chimique de la fibre au fil, PhD Thesis, Université de Haute Alsace-Mulhouse (2012).

[56] R. Siddique, Effect of fine aggregate replacement with Class F fly ash on the abrasion resistance of concrete, Cem. Concr. Res., 33 (2003), pp. 1877-1881, 10.1016/S0008-8846(03)00212-6.

[57] M. Sadegzadeh, R. Kettle, V. Vassou, The influence of glass, polypropylene and steel fibers on the physical properties of concrete, Concrete, 35 (2001), pp. 12-22.

[58] M. Gupta, M. Kumar, Effect of nano silica and coir fiber on compressive strength and abrasion resistance of concrete, Constr. Build. Mater., 226 (2019), pp. 44-50, 10.1016/j.conbuildmat.2019.07.232.

[59] A. Alaskar, H. Alabduljabbar, A.M. Mohamed, F. Alrshoudi, R. Alyousef, Abrasion and skid resistance of concrete containing waste polypropylene fibers and palm oil fuel ash as pavement material, Constr. Build. Mater., 282 (2021) 122681, 10.1016/j.conbuildmat.2021.122681.

[60] S. Ajouguim, M. Stefanidou, K. Abdelouahdi, M. Waqif, L. Saâdi, Influence of treated bio-fibers on the mechanical and physical properties of cement mortars, European Journal of Environmental and Civil Engineering. (2020), pp. 1-15, 10.1080/19648189.2020.1782773.

[61] M.R. Ahmad, B. Chen, S.Y. Oderji, M. Mohsan, Development of a new bio-composite for building insulation and structural purpose using corn stalk and magnesium phosphate cement, Energy Build., 173 (2018), pp. 719-733.

[62] M. Boumhaout, L. Boukhattem, H. Hamdi, B. Benhamou, F. Ait Nouh, Thermomechanical characterization of a bio-composite building material: mortar reinforced with date palm fibers mesh, Constr. Build. Mater., 135 (2017), pp. 241-250.

[63] F. Benmahiddine, R. Cherif, F. Bennai, R. Belarbi, A. Tahakourt, K. Abahri Effect of flax shives content and size on the hygrothermal and mechanical properties of flax concrete, Constr. Build. Mater., 262 (2020), Article 120077, 10.1016/j.conbuildmat.2020.120077.

[64] A. Laborel-Preneron, C. Magniont, J.E. Aubert, Hygrothermal properties of unfired earth bricks: effect of barley straw, hemp shiv and corn cob addition, Energy Build., 178 (2018), pp. 265-278.

[65] L.-M. Sun, F. Meunier, Adsorption: aspects théoriques, Techniques de l'ingénieur (2003).

[66] J.B. Condon, Chapter 3 – Interpreting the Physisorption Isotherm J.B. Condon (Ed.), Surface Area and Porosity Determinations by Physisorption, Elsevier Science, Amsterdam (2006), pp. 55-90.

[67] M. Saidi, A.S. Cherif, B. Zeghmati, E. Sediki, Stabilization effects on the thermal conductivity and sorption behavior of earth bricks, Constr. Build. Mater., 167 (2018), pp. 566-577.

[68] J. Kwiatkowski, M. Woloszyn, J.-J. Roux, Influence of sorption isotherm hysteresis effect on indoor climate and energy demand for heating, Appl. Therm. Eng., 31 (2011), pp. 1050-1057.

[69] R. Belakroum, A. Gherfi, M. Kadja, C. Maalouf, M. Lachi, N. El Wakil, T. Mai, Design and properties of a new sustainable construction material based on date palm fibers and lime, Constr. Build. Mater., 184 (2018), pp. 330-343.